

<https://doi.org/10.1038/s40494-025-02072-4>

Microstructural evolution of Jin Zhuan from the Ming and Qing dynasties at the Yuanhetang kiln site

Check for updates

Yushen He¹✉, Yanhong Li² & Yi Zhou³

This study investigates the unfired and fired microstructural characteristics of Jin Zhuan (imperial bricks) from the Ming–Qing period, using materials excavated from the Yuanhetang kiln site in Suzhou, China. Employing a combination of X-ray diffraction (XRD), scanning electron microscopy coupled with energy-dispersive X-ray spectroscopy (SEM-EDS), and mercury intrusion porosimetry (MIP), the mineralogical composition, microstructural evolution, and porosity changes associated with the imperial brickmaking process were analysed. The unfired samples exhibited a fine-grained, silicate-rich clay body, while the fired bricks showed evidence of significant densification, sintering neck formation, and a more uniform pore network. Comparison with historical texts, such as Zaozhuan Tushuo and Gusu Zhi, highlights the intricate artisanal techniques developed to optimise brick performance. Our findings provide new scientific insights into the material transformations underpinning the renowned durability and quality of Jin Zhuan, offering valuable references for future conservation, heritage reproduction, and material science research.

Fired clay bricks have been present in China since the Neolithic period, with archaeological evidence suggesting their production as early as 5000 years ago¹. However, their widespread structural use did not emerge until the late 3rd century BCE, when brickmaking became institutionalised in architecture^{1,2}.

Imperial bricks known as Jin Zhuan (金砖), often translated as “golden bricks,” were a distinctive category of high-quality fired clay bricks reserved for high-status imperial constructions during the Ming (1368–1644 CE) and Qing (1644–1912) dynasties of China³. Valued for their exceptional density, smooth finish, and distinctive metallic resonance when struck, Jin Zhuan exemplified the aesthetic and technical ideals of imperial craftsmanship—qualities traditionally summarized as “heavy as gold, bright as a mirror, smooth as cream, and sounding like metal and stone”⁴. According to Zaozhuan Tushuo (《造砖图说》, Treatise on Brickmaking) compiled by Zhang Wenzhi, a senior official of the Ministry of Works during the Ming dynasty, the production of Jin Zhuan was formally institutionalized during the Yongle reign (1402–1424 CE), when the imperial court commissioned 63 kiln households in the Lumu area of Suzhou to manufacture bricks for the newly constructed Forbidden City. The text specifies that the bricks had to meet rigorous dimensional standards and be produced exclusively from clay sourced in northeastern Suzhou⁵. Additional records in Gusu Zhi (《姑苏志》, Records of Suzhou) confirm that the bricks from this region were highly regarded for their strength and uniformity⁶. While initially used for

palatial structures, Jin Zhuan later served broader roles in Qing dynasty architecture, including temples, government buildings, elite residences, and ornamental gardens³. These historical sources provide detailed accounts of sourcing, sedimentation, forming, and firing techniques, especially in Zhizhuantu (《制砖图》, Illustrated Manual of Brickmaking), an illustrated manual associated with Zaozhuan Tushuo. As a visual supplement to the text, this manual vividly demonstrates the systematic and technically refined nature of imperial brick production⁵.

Although richly documented in historical records, Jin Zhuan has rarely been examined through modern scientific approaches. Most existing studies focus on archival texts, traditional craft manuals, and oral accounts from contemporary practitioners^{3–6}, with limited attention to their physical, mineralogical, or microstructural properties. To date, the only known scientific investigation of Jin Zhuan is the 1989 study by Yang Wuhua et al., which analysed bricks from the Forbidden City using basic compositional and physical methods. Their study concluded that the material was incompletely sintered, with relatively low porosity and good density, and was composed of processed, fine-grained clay⁷. However, this pioneering study was limited to finished products and did not examine the transformation of material structure during firing. Existing studies on historical bricks have addressed a range of technical aspects, including their chemical composition^{8–21}, microstructure^{11,14–23}, mechanical performance^{10,18–20,23}, weathering mechanisms¹⁷, provenance and raw material sourcing^{12–15,20,21},

¹University of Oxford, Oxford, UK. ²Henan Provincial Institute of Cultural Relics and Archaeology, Zhengzhou, China. ³Chifeng University, Chifeng, China.

✉ e-mail: hys6006@163.com

surface features and coatings^{21,24}, and firing technology and thermal behaviour^{12,14,15,17,18,20,22}. However, comparative analyses incorporating both unfired and fired brick samples within a single production sequence remain largely absent.

Recent excavations at the Yuanhetang kiln site in Suzhou have provided a rare opportunity to address this gap. The site, covering 1,618 m² and divided into four excavation areas, yielded 48 features, including 12 kilns, drying areas, sedimentation pits, brick roads, and other associated structures. It produced both well-preserved unfired brick bodies from drying areas and fired Jin Zhuan samples from kiln remains, enabling a direct comparative study of raw and finished materials within the same production sequence. This study applies three widely adopted techniques in the analysis of historical bricks: X-ray diffraction (XRD)^{7–24}, scanning electron microscopy (SEM)^{11,12,14,16–24}, and mercury intrusion porosimetry (MIP)^{16–20,23}, to investigate mineralogical composition, microstructural features, and pore system evolution. By combining these methods, this study aims to reveal the microstructural mechanisms that drive densification and porosity evolution in imperial brickmaking, thereby contributing new scientific insight into the technological complexity behind this enduring craft tradition.

Methods

Sample collection and preparation

All samples were collected from the Yuanhetang kiln site, located in the Lumu area of Suzhou, Jiangsu Province, China. This site, excavated in 2021–2022 by the Suzhou Institute of Archaeology, is a Ming dynasty kiln site where Jin Zhuan were produced. The excavation uncovered kilns, sedimentation pits, ash pits, and a drying area that preserved unfired brick blanks. The co-occurrence of unfired and fired bricks at the site offers a valuable opportunity for comparative study.

The unfired sample used in this study was taken from the drying area. To avoid surface contamination, the outer layer was removed and material was collected from deeper interior portions. The fired Jin Zhuan sample was collected from nearby kiln remains for comparative analysis. Representative images of the sampling context are shown in Fig. 1.

X-ray diffraction (XRD) analysis

X-ray diffraction was conducted to identify the crystalline phases present in the samples. The analysis was performed using a D/max-rB 12 kW powder

diffractometer with the following conditions: tube voltage of 40 kV, tube current of 100 mA, graphite monochromator, $\theta/2\theta$ scanning mode, scan speed of 8° (2 θ) per minute, and a step size of 0.02° (2 θ). Measurements were carried out at room temperature (24 °C) and a relative humidity of 50%.

Scanning electron microscopy (SEM-EDS)

Microstructural features were examined using an FEI Quanta 200 FEG (FEI, USA) under high vacuum. The fired sample was imaged at 15.0 kV (working distance 14.2 mm, spot size 4.0); the unfired sample at 10.0 kV (working distance 14.5 mm). Both micrographs were acquired at a nominal magnification of 2000 \times . Energy-dispersive X-ray spectroscopy (EDS) was used to qualitatively assess elemental composition.

Mercury intrusion porosimetry (MIP)

Mercury intrusion porosimetry was employed to investigate pore size distribution and total porosity. This technique provides quantitative data on the internal pore structure of porous materials and is widely used in the study of historic building materials. A Quanta Chrome AutoScan-33 porosimeter was used for the measurements.

Results

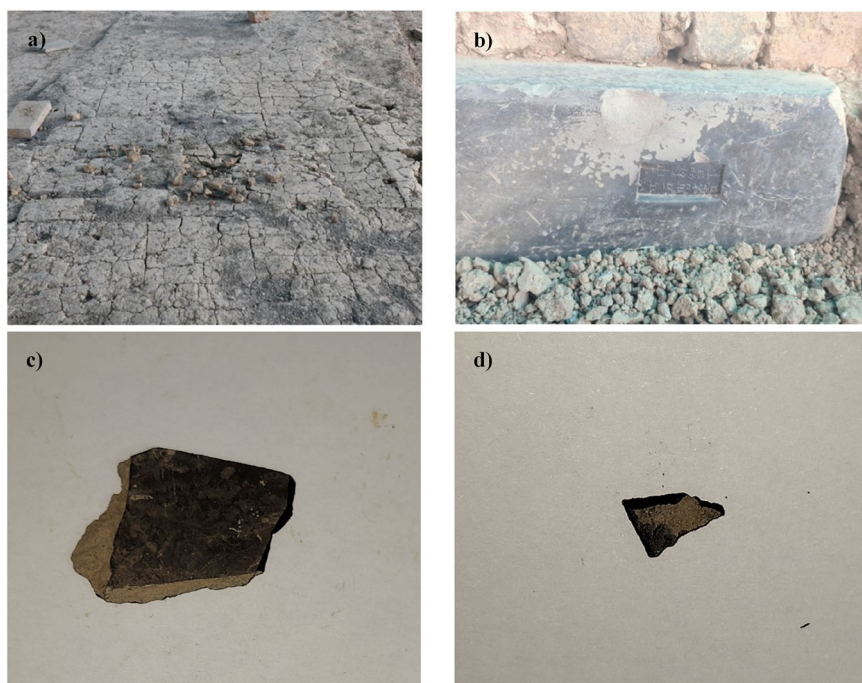
Mineralogical characteristics of the unfired sample

XRD analysis of the unfired brick sample (Supplementary Fig. 1) identified quartz as the dominant mineral phase, accompanied by notable amounts of montmorillonite and minor feldspars (Table 1). This composition is characteristic of a fine-grained, silicate-rich clay body suitable for imperial brickmaking. The presence of montmorillonite is particularly significant, as it is known to enhance both the plasticity and green strength of raw clay materials, improving their overall workability and structural stability prior to firing²⁵. Feldspar and calcite, though present in limited quantities, are common constituents of natural soil.

According to Zaozhuan Tushuo, clay used for Jin Zhuan was sourced exclusively from the Lumu region northeast of Suzhou, where a distinctive dry yellow soil was prized for its performance. The treatise describes an elaborate multistage refinement process, including sun-drying, pounding, sieving, levigation through tiered settling pools, and extended shade-drying and compaction over several months prior to shaping⁵. These procedures, though based on empirical practice rather than compositional theory,

Fig. 1 | Site context and representative samples analysed in this study. **a** Unfired brick blanks exposed in situ at the drying yard of the Yuanhetang kiln site. **b** Fired imperial brick (Jin Zhuan) bearing an official stamp, excavated from the same context.

c Representative unfired brick sample. **d** Representative fired brick sample. Scale bars in (c) and (d) are estimated from sample dimensions.



appear to have effectively concentrated the fine-grained fraction and minimised deleterious inclusions, resulting in a clay body composition well suited to the strict forming, drying, and firing demands of imperial brickmaking.

Table 1 | Mineralogical composition of the unfired brick sample based on XRD analysis

Mineral phase	PDF card	Estimated wt.% (±)
Quartz	PDF#01-075-0443	63.3 ± 0.9
Montmorillonite	PDF#00-029-1499	17.8 ± 0.4
Albite	PDF#01-071-3816	7.8 ± 0.2
Microcline	PDF#00-019-0932	5.9 ± 0.2
Illite	PDF#00-026-0911	3.3 ± 0.1
Calcite	PDF#01-086-4274	1.9 ± 0.1

Structural evolution during firing

This study systematically revealed the microstructural transformation, elemental composition, and pore characteristics of Jin Zhuang samples during firing. The combination of SEM, EDS, and MIP techniques allowed visualisation of the densification process and quantitative analysis of microstructural reorganisation.

The unfired sample showed a loosely packed, sheet-like, and highly porous structure under SEM (Fig. 2a), with distinct grain boundaries and little evidence of continuous contacts or neck formation, indicating relatively low mechanical strength and stability. EDS analysis (Fig. 2b) identified O, Si, and Al as the principal elements, with minor K, Na, Ca, and Fe, characteristic of typical clay mineral compositions. In contrast, the fired sample exhibited markedly different features (Fig. 2c), including well-developed sintering necks, blurred grain boundaries, and partial particle coalescence, forming a more continuous and cohesive microstructure. EDS analysis (Fig. 2d) showed a similar elemental profile, dominated by O, Si, Al, Fe, K, Na, and Ca. These microstructural and compositional changes suggest that the firing process transformed the material from a loosely aggregated

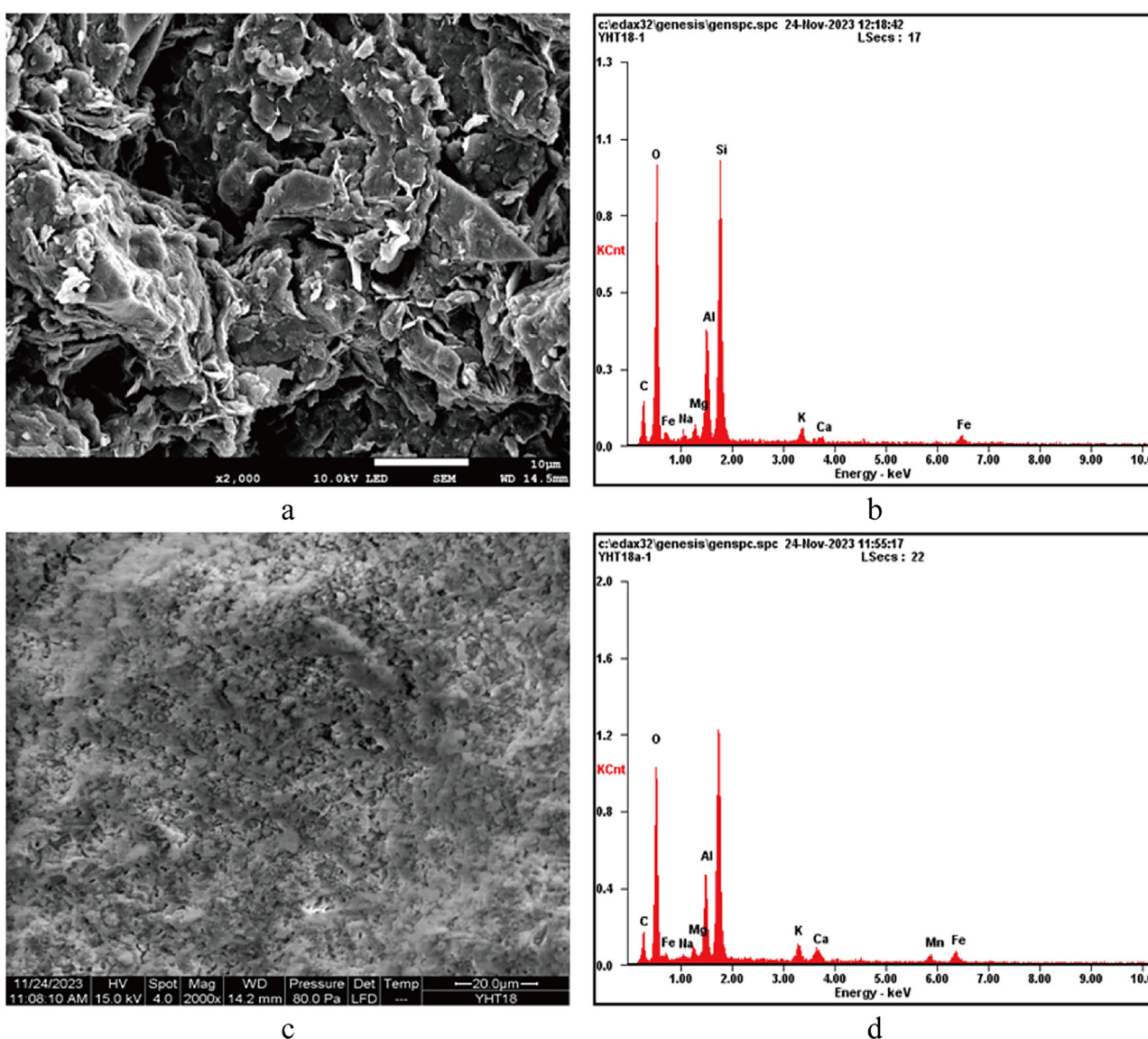
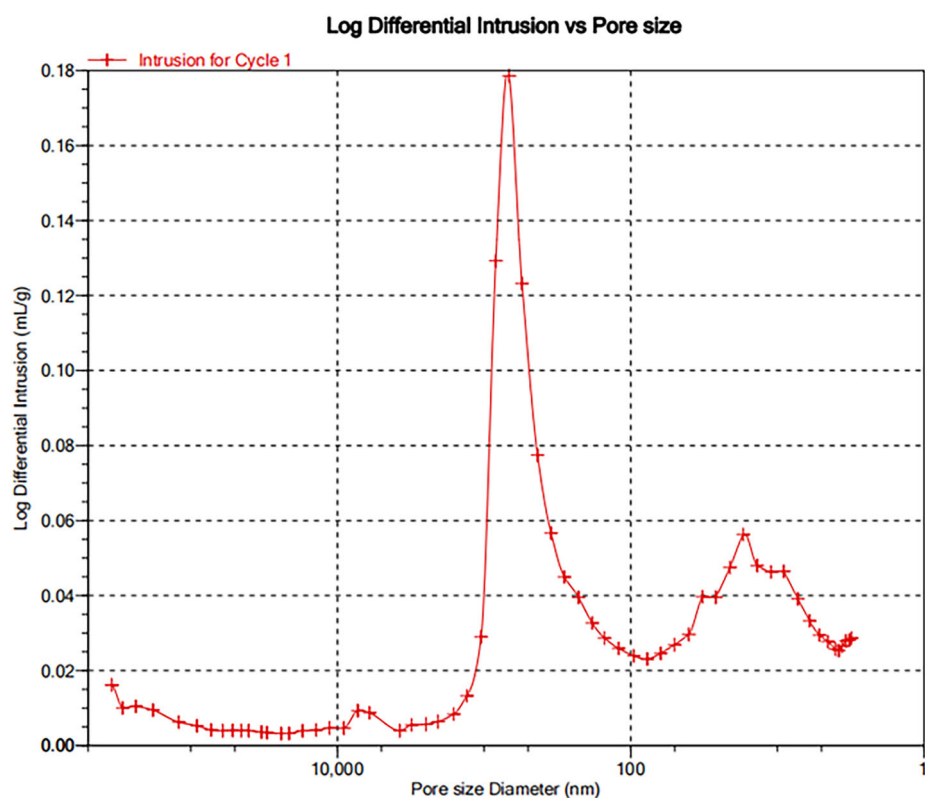


Fig. 2 | SEM and EDS analyses of the unfired and fired Jin Zhuang samples. a SEM image (2000×) of the unfired sample. **b** EDS spectrum of the unfired sample. **c** SEM image (2000×) of the fired sample. **d** EDS spectrum of the fired sample. Although both SEM images were acquired at a nominal magnification of 2000×, they were

collected in separate sessions on different instruments, leading to differences in field of view and on-image scale. Accordingly, morphological comparisons are qualitative, focusing on particle packing, pore structure, and grain-size distribution.

Fig. 3 | Log differential intrusion versus pore size of the unfired Jin Zhuuan sample. The curve exhibits a bimodal distribution with peaks at approximately 300–400 nm, 40–50 nm, and 10–20 nm, indicating a multi-scale pore network formed during shaping. The x-axis (pore diameter, in nm) and y-axis (log differential intrusion volume) are shown for clarity. Quantitative data for porosity and average pore diameter are provided in Supplementary Table 1.



particle body into a densely sintered matrix, thereby improving its density and mechanical performance.

MIP analysis (Figs. 3 and 4) provided quantitative confirmation of these observations. The unfired sample (Fig. 3) had a total porosity of approximately 26.5% and an average pore diameter of around 28.8 nm (Supplementary Table 1). Its log differential intrusion versus pore size curve displayed a distinct bimodal distribution, with a primary peak near 300–400 nm and secondary peaks at 40–50 nm and 10–20 nm, reflecting a multi-scale pore network formed during shaping. In contrast, the fired sample (Fig. 4) showed a slightly reduced total porosity (25.3%) and an increased average pore diameter (42.8 nm) (Supplementary Table 1). Its differential intrusion curve presented a single dominant peak, with sharply reduced secondary peaks. This suggests that the firing process involved the collapse of larger pores and reorganisation of the fine-pore system, leading to a more uniform pore distribution. Despite the slight increase in average pore diameter, the overall reduction in porosity and the homogenisation of the pore network contributed to enhanced densification and mechanical strength. These findings are consistent with the SEM-EDS observations (Fig. 2), jointly revealing the key physical mechanisms underlying Jin Zhuuan's performance improvements during firing.

In summary, the SEM-EDS and MIP tests revealed the microstructural evolution, pore reorganisation, and densification mechanisms occurring during the firing of Jin Zhuuan. These insights enrich our understanding of the microstructural performance of ancient architectural materials and provide a scientific foundation for future research on process optimisation, conservation strategies, and long-term durability assessment.

Discussion

The production of Jin Zhuuan, or imperial bricks, has long been a symbol of technical mastery and cultural heritage. Historical texts, such as the *Zaozhuan Tushuo*⁵ and detailed artisanal records³, describe a meticulously structured production process encompassing over twenty interlocking stages. According to the *Zaozhuan Tushuo*, this process involved seven cycles of clay preparation (sun-drying, pounding, grinding, sieving) and six

cycles of mud refinement (settling, filtering, layering, smoothing, binding, treading), followed by manual shaping, prolonged slow drying for up to eight months, and a carefully staged firing regime lasting over 130 days. The firing sequence used successive fuels—such as rice husks, twig wood, and pine branches—to gradually raise the temperature and induce controlled phase changes. After firing, the bricks underwent water curing, polishing, oiling, and strict inspection, with only the whitest, most flawless bricks passing the imperial standards^{3,5,6}. These intricate practices were designed to maximise densification, reduce porosity, and enhance mechanical performance. Our experimental results, particularly the identified low-calcium, silica- and alumina-rich compositions, sintering neck formation, and reduced pore connectivity, align well with these historical processes, underscoring the deep empirical knowledge embedded in traditional craftsmanship. These compositional features laid the foundation for the subsequent thermal transformation processes, which are examined below through structural and porosity analysis.

While these historical insights are valuable, earlier scientific investigations have also provided foundational comparative data for understanding the properties of imperial bricks. Previous research, notably the work by Yang et al.⁷, provided foundational insights into the chemical compositions, mineral phases, and physical properties of imperial bricks. Yang's XRD analysis identified quartz, feldspar, and mica as principal crystalline phases in fired bricks from the Forbidden City, with no residual clay minerals observed. While their provenance remains uncertain, these bricks are documented to have been used in imperial construction, and their mineralogical features offer qualitative reference points. Yang also reported an open porosity of approximately 27.3%, accompanied by high compressive strength and durability. Our study complements and extends this prior work by applying MIP to quantify not only the total porosity (25.3%) but also the average pore size, pore size distribution, and structural evolution during firing. For the fired samples, the total porosity measured in this study is noticeably lower than the open porosity reported by Yang. Given that total porosity generally exceeds open porosity, this suggests a higher degree of densification in our samples. However, this difference likely reflects

Fig. 4 | Log differential intrusion versus pore size of the fired Jin Zhuan sample. A single dominant peak is observed, with significantly reduced secondary peaks, indicating a more uniform pore structure after firing. Axes represent pore diameter (nm) and log differential intrusion volume. Corresponding values for porosity and average pore diameter are detailed in Supplementary Table 1.

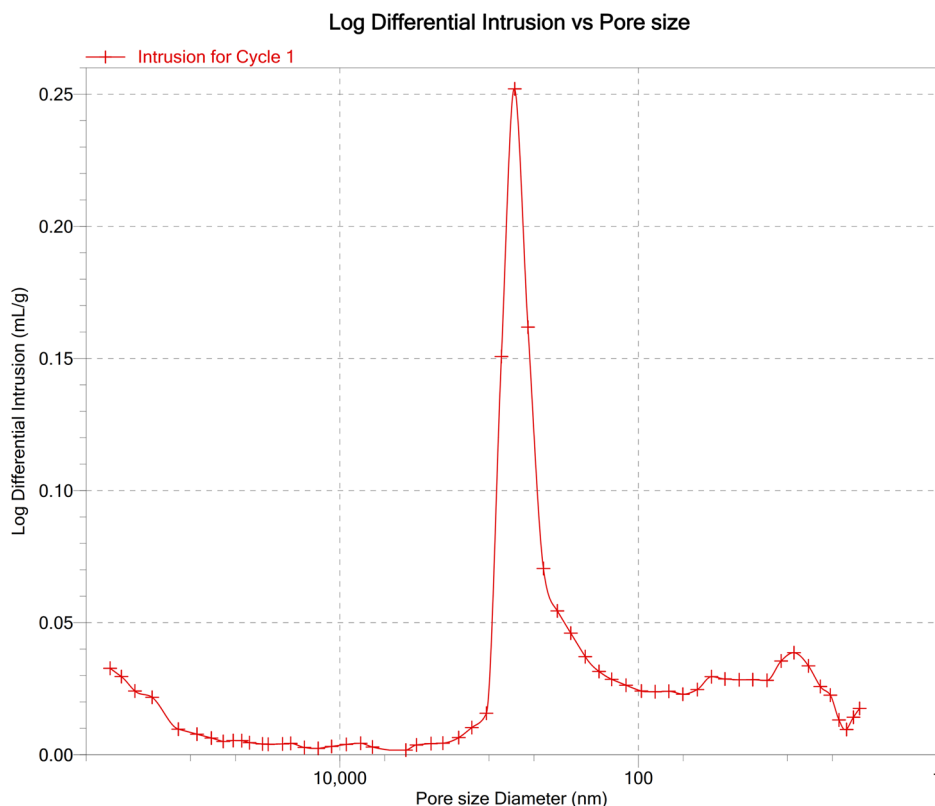


Table 2 | Comparative porosity data for Jin Zhuan and fired bricks from similar periods reported in previous studies

Period	Location	Building type	Sample number	Porosity/%	Method	Reference
Ming	Xi'an	City wall	1	19.2	MIP (Total porosity)	16
Qing	Xi'an	City wall	4	19.3–21.9	MIP (Total porosity)	16
Ming	Nanjing	City wall	6	37.3	Water saturation method (Open porosity)	18
Ming	Nanjing	City wall	5	30.9	Water saturation method (Open porosity)	18
Ming	Xi'an	City wall	4	32.6	Water saturation method (Open porosity)	18
Ming	Linqing	City wall	2	40.0	Water saturation method (Open porosity)	18
Ming	Beijing	City wall	3	41.6	Water saturation method (Open porosity)	18
Ming	Nanjing	City wall	2	34.7–35.3	MIP (Total porosity)	19
Qing	Yichun	Residential building	2	37.4–41.3	MIP (Total porosity)	19
Qing	Suzhou	Residential building	1	31.1	MIP (Total porosity)	19
Ming-Qing	Suzhou	Royal building	2	25.3(unfired 26.5)	MIP (Total porosity)	[This study]

variations in provenance, historical production techniques, and material formulations, rather than solely the firing process itself. These findings highlight the importance of further comparative studies on bricks from different kiln sites to better understand the technological details and optimise conservation strategies.

The porosity of the Jin Zhuan analysed in this study was also compared with values reported for fired bricks from similar historical periods (Table 2). Overall, the Jin Zhuan shows lower porosity than most contemporaneous wall bricks compiled here, which is consistent with a higher degree of densification. Note that the literature values include both open porosity measured by the water-saturation method and total porosity from MIP; these metrics are not strictly comparable, so the comparison is intended to be indicative rather than definitive. When considered alongside the SEM/EDS and MIP observations in this study, these comparative porosity patterns indicate stronger densification in Jin Zhuan than in ordinary wall bricks, motivating the broader implications discussed below.

From a broader perspective, these microstructural insights not only validate the effectiveness of traditional craftsmanship but also deepen our understanding of the relationship between material science and cultural heritage. By bridging the gap between experimental data and historical documentation, this research offers valuable guidelines for the restoration of heritage sites, the reproduction of authentic materials, and the preservation of intangible artisanal knowledge.

This study compared unfired and fired brick samples from the Yuanhetang site through XRD, SEM/EDS, and MIP analyses. The fired Jin Zhuan exhibited lower porosity and a denser microstructure than most contemporaneous wall bricks reported in the literature, reflecting deliberate firing practices aimed at achieving high strength and durability. These results align with historical records of standardised production in the Ming–Qing imperial brickmaking system, illustrating how technical precision was embedded within state-controlled manufacture. Importantly, the underlying principles—careful raw material selection, controlled firing

regimes, and densification strategies—remain relevant today and could inform the design of durable, low-porosity masonry for sustainable modern construction, particularly in contexts demanding high weathering resistance and minimal maintenance. Nonetheless, the absence of direct thermal expansion data constrains the precision of firing temperature estimates, and the focus on a single fired–unfired pair from one production site leaves potential regional variability and statistical robustness unaddressed; in the future, expanding the dataset to include multiple specimens from other kilns, as well as controlled experimental firings, would help refine these interpretations.

Data availability

All data generated or analysed during this study are included in this published article and its supplementary information file.

Received: 28 May 2025; Accepted: 23 September 2025;

Published online: 16 October 2025

References

1. Yang, Y., Yu, S., Zhu, Y. & Shao, J. The making of fired clay bricks in China some 5000 years ago. *Archaeometry* **56**, 220–227 (2014).
2. Nickel, L. Bricks in Ancient China and the question of early cross-Asian interaction. *Arts Asiatiques* **70**, 49–62 (2015).
3. Ji H. Suzhou yuyao jinzhuan ji qi zhizuo jiji [Suzhou imperial kiln golden bricks and their manufacturing techniques]. Jiangsu Difangzhi. 8–11 (2012) (in Chinese).
4. Gu, X. Chengni zaozhuan—qiantan yuyao jinzhuan qu tu [Clay preparation for imperial golden bricks: A brief discussion on the use of Chengni clay]. Taoci. 75–77 (2017) (in Chinese).
5. Zhang, W. Zaozhuan Tushuo [Treatise on Brickmaking]. Edited by Jin J., Zhou Z. L. Yangzhou: Guangling Shushe; (2020) (in Chinese).
6. Wang A. Gusu Zhi [Records of Suzhou]. In: Beijing Tushuguan Guji Zhenben Congkan, 27. Beijing: Shumu Wenxian Chubanshe; (1998) (in Chinese).
7. Yang, W., Xu, N., Miao, S. & Xu, X. Gudai “jinzhuan” de yanjiu [Study on ancient imperial bricks]. Zhongguo Taoci. 57–61 (1989) (in Chinese).
8. de Oliveira, L. M. G., de Oliveira Freire, F. L., Ribeiro, F. R. C., Sousa, I. N. L., Mesquita, E. & Bertini, A. A. Investigation of the mortars and clay bricks of a luso-brazilian historic structure from XVIII century: The Nosso Senhor do Bonfim Church. *J. Build. Eng.* **45**, 103592 (2022).
9. Lanphear, K. M. Profile of an origin: A chemical and physical characterization study of historic brick and clay from the Ashley River, South Carolina. M.S. Thesis. Clemson University (2011).
10. Galindo, J., Paredes, J. & Muñoz, A. Estudio y caracterización de los ladrillos de un puente histórico en Buga (Valle del Cauca) / Study and characterization of bricks from a historical bridge in Buga (Valle del Cauca). Revista Facultad de Ingeniería. Univ. de. Antioquia **48**, 130–140 (2009) (in Spanish).
11. Schiavon, N., Mazzocchin, G. A. & Baudo, F. Chemical and mineralogical characterisation of weathered historical bricks from the Venice lagoonal environment. *Environ. Geol.* **56**, 767–775 (2008).
12. Mishra, A. K. & Mishra, A. Geochemical characterization of bricks used in historical monuments of 14–18th century CE of Haryana region of the Indian subcontinent: Reference to raw materials and production technique. *Constr. Build. Mater.* **269**, 121802 (2021).
13. Asfora, V. K., Bueno, C. C., de Barros, V. M., Khoury, H. & Van Grieken, R. X-ray spectrometry applied for characterization of bricks of Brazilian historical sites. *X-Ray Spectrom.* **50**, 45–52 (2021).
14. Bianchini G., Marrocchino E., Moretti A. & Vaccaro C. Chemical-mineralogical characterization of historical bricks from Ferrara: an integrated bulk and micro-analytical approach. In: Maggetti M., & Messiga B. (eds) *Geomaterials in Cultural Heritage*. (Geological Society, London, Special Publications. 257:127–140 2006).
15. Bolognesi, E., Fabbri, B., Macchiarola, M. & Kotas, P. Characterisation of historic bricks from the ruins of the great imperial palace in Istanbul. *Key Eng. Mater.* **264**, 2383–2386 (2004).
16. Li, C., Wu, C., Gao, H., Wang, S., Guo, Y., Chen, Y. & Jin, P. Chemical and microscopic investigation of historical wall bricks collected from the City Wall of Xi'an, China. *J. Cult. Herit.* **64**, 144–149 (2023).
17. An, L., Qiao, Z., Wang, J. & Wang, F. Experimental study on weathering mechanism of ancient bricks in Jiayuguan Wei-Jin tombs, Gansu, China. *Herit. Sci.* **12**, 114 (2024).
18. Shi, J., Chun, Q., Mi, Z., Feng, S., Liu, C., Liu, Z., Wang, D. & Zhang, Y. Comparative study on material properties of ancient fired clay bricks of China. *Case Stud. Constr. Mater.* **19**, e02463 (2023).
19. Chun, Q., Dong, Y., van Balen, K. & Xu, X. Experimental research on material properties of ancient white bricks in the Yichun Region, China. *Int. J. Archit. Herit.* **11**, 554–565 (2017).
20. Qi, G., Wang, D., Xu, D., Zhang, D., Wang, Q., Tang, Y. & Zhu, Y. Analysis of lime paste and bricks from the Ming Dynasty: Composition, structure, properties, and adhesion mechanism. *Constr. Build. Mater.* **461**, 139929 (2025).
21. Han, W., Pei, S. & Liu, F. Material characterization of the brick in the Ming Dynasty heritage wall of Pianguan County: A case study. *Case Stud. Constr. Mater.* **16**, e00940 (2022).
22. López-Arce, P., García-Guinea, J., Gracia, M. & Obis, J. Bricks in historical buildings of Toledo City: characterisation and restoration. *Mater. Charact.* **50**, 59–68 (2003).
23. Manohar, S., Shukla, S., Menon, A. & Santhanam, M. Characterization of historic bricks and binder at Vat Phou World Heritage Site in Lao PDR and selection of compatible replacement units for restoration. *Curr. Sci.* **119**, 1300–1307 (2020).
24. Zhou, S., He, Y., Li, Y., Wang, B. & Yang, R. The preliminary analysis of the decorated bricks in the chamber of the Northern Wei Jing Ling site in Luoyang. *J. Archaeol. Sci.: Rep.* **61**, 104949 (2025).
25. Murray, H. H. Traditional and new applications for kaolin, smectite, and palygorskite: a general overview. *Appl. Clay Sci.* **17**, 207–221 (2000).

Acknowledgements

This study received no funding. The authors thank the Suzhou Institute of Archaeology for site access and sampling permission.

Author contributions

Y.H. conceived the research, designed the methodology, conducted the experiments, analysed the data, and wrote the manuscript. Y.L. contributed to data interpretation and manuscript revision. Y.Z. assisted with analytical methods and provided critical feedback. All authors reviewed and approved the final version.

Competing interests

The authors declare no competing interests.

Additional information

Supplementary information The online version contains supplementary material available at <https://doi.org/10.1038/s40494-025-02072-4>.

Correspondence and requests for materials should be addressed to Yushen He.

Reprints and permissions information is available at <http://www.nature.com/reprints>

Publisher's note Springer Nature remains neutral with regard to jurisdictional claims in published maps and institutional affiliations.

Open Access This article is licensed under a Creative Commons Attribution-NonCommercial-NoDerivatives 4.0 International License, which permits any non-commercial use, sharing, distribution and reproduction in any medium or format, as long as you give appropriate credit to the original author(s) and the source, provide a link to the Creative Commons licence, and indicate if you modified the licensed material. You do not have permission under this licence to share adapted material derived from this article or parts of it. The images or other third party material in this article are included in the article's Creative Commons licence, unless indicated otherwise in a credit line to the material. If material is not included in the article's Creative Commons licence and your intended use is not permitted by statutory regulation or exceeds the permitted use, you will need to obtain permission directly from the copyright holder. To view a copy of this licence, visit <http://creativecommons.org/licenses/by-nc-nd/4.0/>.

© The Author(s) 2025